THE JOURNAL OF COMPARATIVE NEUROLOGY 376:386–402 (1996)

Phenotypic Characterisation of Respecified Visual Cortex Subsequent to Prenatal Enucleation in the Monkey: Development of Acetylcholinesterase and Cytochrome Oxidase Patterns

COLETTE DEHAY, PASCALE GIROUD, MICHEL BERLAND, HERBERT P. KILLACKEY, AND HENRY KENNEDY
INSERM U371 (C.D., P.G., H.K.), Cerveau et Vision, Cedex, France, and Centre Hospitalier Lyon Sud (M.B.), Cedex, Pierre Bénite, France; Department of Psychobiology (H.P.K.), University of California, Irvine, California, 96297-4550

ABSTRACT

Prenatal bilateral enucleation induces cortex, which normally would have become striate cortex, to follow a default developmental pathway and to take on the cytoarchitectonic appearance of extrastriate cortex (default extrastriate cortex, Dehay et al. [1996] J. Comp. Neurol. *367*:70–89). We have investigated if this manipulation influences the cortical expression of acetylcholinesterase (AChE) and cytochrome oxidase (CO).

Early enucleation (before embryonic day 81; E81) had only minor effects on the distribution of AChE and CO in the striate cortex. In animals that underwent operation, the striate cortex CO blobs were significantly more closely spaced on the operculum compared with the calcarine.

After early enucleation, there was a periodic distribution of CO dense patches in default extrastriate cortex. These CO patches had a center-to-center spacing that was considerably smaller than that of CO stripes in normal area V2, but was somewhat larger than that of the CO blobs in striate cortex. Although the CO stripes characteristic of normal area V2 could not be detected, there were some high-frequency CO patches, similar to those found in default extrastriate cortex.

Early enucleation caused a failure to form the transient AChE bands running perpendicular to the striate border, which are normally present in the fetus and early neonate. Late enucleation did not alter AChE expression in extrastriate cortex.

The relatively minor effects of early enucleation in the reduced striate cortex contrast with the changes in expression of these enzymes in extrastriate cortex, which accompany large shifts in the location of the striate border. This suggests a massive reorganisation of cortical phenotype in extrastriate cortex.

Indexing terms: primate, plasticity, vision, striate cortex, extrastriate cortex

The presence of the retinae during prenatal development is essential for the normal specification of the dimensions of monkey striate cortex (Rakic, 1988; Dehay et al., 1989, 1991, 1996; Rakic et al., 1991). Early fetal bilateral enucleation (before embryonic day 81; E81) leads to a reduction in the dimensions of area 17 which, however, retains its normal lamination. Quantitative measurements of different cortical regions have provided evidence that this large reduction of striate cortex is accompanied by an expansion of extrastriate cortex (Dehay et al., 1996). These results support the conclusion that early enucleation leads to a border shift and that cortex immediately surrounding the reduced striate cortex was destined to become striate cortex. This amounts to the respecification of a cortical area and is, therefore, of considerable theoretical interest. However, the cortex immediately surrounding the reduced striate cortex in the early enucleate has a cytoarchitecture indistinguishable from that of the extrastriate cortex in the

Accepted July 12, 1996.

Address reprint requests to Henry Kennedy, INSERM U371, 18 Av Doyen Lépine, 69675 Bron, Cedex, France. E mail:kennedy@Lyon151.inserm.fr

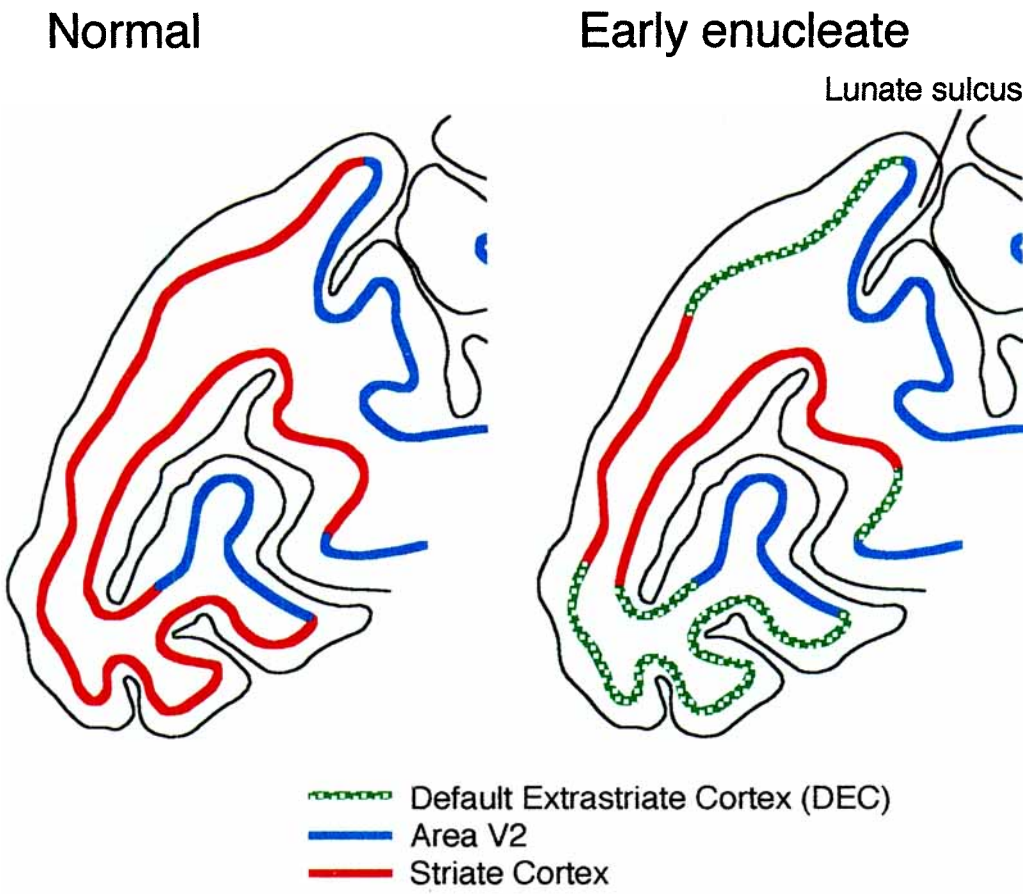

Fig. 1. Effect of early enucleation (before embryonic day 81, E81) on the dimensions of striate cortex and the location of default extrastriate cortex (DEC). In the normal animal, striate cortex is surrounded by area V2 as shown in this parasaggital section. Similar sections in an early enucleate demonstrate that striate cortex is considerably reduced. Areal measurements show that the overall dimensions of the neocortex are not influenced by enucleation, so that the cortex that was destined to become striate cortex takes on an cytoarchitecture that is indistinguishable from area 18, and this region is referred to as DEC. Although we do not know the exact dimensions of DEC, we can assume that it extends as far as the limits of striate cortex in the normal animal. DEC can be expected to be, in turn, surrounded by presumptive area V2.

lunate sulcus in both early enucleated animals and normal controls (Dehay et al., 1996). In our earlier work (Dehay et al., 1996), we argued that in the absence of peripheral cues, cortex originally destined to become striate cortex follows an alternative, default developmental course leading to a cytoarchitectonic organisation largely indistinguishable from that of area 18. Hence, in the present study, we shall refer to cortex that has switched phenotypes in this way as default extrastriate cortex (DEC; Fig. 1).

The early enucleation preparation allows an examination of the developmental definition of a cortical area. Do those mechanisms that establish the cytoarchitectonics of a cortical area also determine other phenotypic attributes such as the histochemical organisation? If there is phenotypic constancy, one would predict that the reduced striate cortex would exhibit those phenotypic features normally found in this area, whereas DEC would exhibit those features normally found in area 18. We have addressed this issue by assaying the development of acetylcholinesterase (AChE) and cytochrome oxidase (CO) activity after fetal enucleation in the monkey and focusing on three experimental issues.

First, the effects of enucleation on the formation of the striate border. During normal development, the cytoarchitectonic border of the striate cortex emerges toward the end of cortical neurogenesis at E100. The border of striate cortex is remarkably sharp, and two-dimensional reconstructions show that striate cortex is a compact area with smooth continuous contours (Van Essen and Maunsell, 1980; Dehay et al., 1996). In the early enucleate, the border between striate cortex and DEC is not continuous. Instead, there are indentations of the border and occasional islands of DEC near the periphery of the reduced striate cortex (Dehay et al., 1996). These observations suggest that the developmental mechanisms that underlie interareal border formation break down following early enucleation. One would expect these mechanisms to be related to those establishing the area-specific patterns of AChE and CO activity. We have, therefore, paid particular attention to the distribution and intensity of AChE and CO activity in the region of the striate border.

Second, the effects of enucleation on the functional architecture of striate cortex. Thalamic input and cortical output are restricted to particular layers and sublayers that can, in part, be identified by their CO labeling (Hubel and Wiesel, 1972; Lund and Boothe, 1975; Hendrickson, 1978; Livingstone and Hubel, 1982; Blasdel and Lund, 1983; Fitzpatrick et al., 1983; Livingstone and Hubel, 1984;

Livingstone and Hubel, 1987; Nakamura et al., 1993; Levitt et al., 1994). The pattern of CO blobs in supragranular layers is related to the functional architecture of the cortex (see Martin, 1988, for review). After early enucleation, CO blobs are present in striate cortex, suggesting that CO blob formation occurs in the absence of any instruction from the retina (Dehay et al., 1989; Kuljis and Rakic, 1989; Kennedy et al., 1990). However, the reduction of striate cortex is nearly five times greater on the opercular surface (which subserves central vision in the normal animal) than within the calcarine fissure (Dehay et al., 1996). This has prompted us to examine CO blob frequency in the reduced striate cortex to determine the effect of this early manipulation on CO blob frequency on the operculum and in the calcarine.

Three, the effects of enucleation on the development of extrastriate cortex. During prenatal development and up until 5 months postnatally, AChE is expressed transiently in area V2 (Barone et al., 1994a). Because the level of transient activity of this enzyme is high, its histochemistry is particularly suitable for a developmental study such as this. In the normal young animal, AChE activity in area V2 forms thick bands running perpendicular to the V1 border. These transient AChE bands have a periodicity that is approximately half that of the CO bands. Serial reconstructions of alternating sections reveal that the AChE bands overlap with the thin and pale CO bands, whereas the interbands overlap with the thick CO bands (Barone et al., 1994b, 1996). It is known that the thickness of CO bands distinguishes adjacent cortical territories with segregated output constituting distinct functional streams (Ungerleider and Mishkin, 1982; Livingstone and Hubel, 1988; Zeki and Shipp, 1988). These results show that AChE bands demarcate area V2 territories that project to area V4, whereas the interbands demarcate the territory projecting to area V5 or MT (DeYoe and Van Essen, 1985; Shipp and Zeki, 1985, 1989; Nakamura et al., 1993; Barone et al., 1996).

The major cortical input to the upper layers of area V2 stems from striate cortex. Although the CO compartments in striate cortex of the early enucleate remain remarkably intact, the 70% reduction of this area should theoretically result in a partial deafferentation of area V2. This raises the question of whether enucleation will influence AChE band formation in area V2 and whether the induced DEC will exhibit these bands.

MATERIALS AND METHODS

The present study is based on observations following bilateral enucleation carried out in nine monkey fetuses. Two cases were examined before birth (at E137 and E155). Three normal neonates and one fetus (E122) served as controls (Table 1). The 10 timed pregnant cynomolgus monkeys (*Macaca irus*) received atropine (1.25 mg, i.m.), dexamethasone (4 mg, i.m.), isoxsuprine (2.5 mg, i.m.), and chlorpromazine (2 mg/kg, i.m.) surgical premedication. They were prepared for surgery under ketamine hydrochloride (20 mg/kg, i.m.) anesthesia. The monkeys were then intubated, and anesthesia was continued with 1% halothane in a N_2O/O_2 mixture (70/30). The heart rate was monitored, and the expired $C0_2$ maintained between 5% and 6%. Body temperature was maintained by using a thermostatically controlled heating blanket. A midline abdominal incision was made, and uterotomy was performed. Between E59 and E110, the fetal head was exposed, bilateral eye removal performed, and the fetus replaced in the uterus after closing incisions. The mother was returned to her cage and given an analgesic (visceralgine, 1.25 mg, i.m.) twice daily for 2 days. In three cases, the fetuses were delivered by cesarian section. The other fetuses were left until term on E165 (Table 1). The animals were anesthetised with ketamine (20 mg/kg, i.m.) followed by a lethal dose of Nembutal (60 mg/kg, i.p.) and perfused through the heart with a 1.25% paraformaldehyde and 1.5% glutaraldehyde solution. After fixation, perfusion was continued with a 10–30% sucrose solution to provide cryoprotection of the brain. Parasagittal sections (60-μm thick) were cut on a freezing microtome. Alternate sections were stained for Nissl substance, CO (Wong-Riley, 1979), and AChE (Hardy et al., 1976). In each animal, several sections were processed for AChE in the presence of eserine, an inhibitor of cholinesterases, to test staining specificity.

TABLE 1. Ages of Monkeys and Procedures Used[1]

Case		Age at observation	CO	AchE
BB3	Normal	P0	X	
BB9	Normal	P0	X	
BB25	Normal	P0	X	X
BB31	Normal	E122	X	X
	Age at enucleation	Age at observation	CO	AchE
BB20	E110	P0	X	
BB26	E91	P0	X	X
BB35	E81	P0	X	X
BB21	E77	P0	X	X
BB28	E68	P0	X	X
BB95	E62	E155		X
BB104	E62	E137		X
BB46	E59	P0	X	X
BB122	E58	P27	X	X

[1]CO, cytochrome oxydase; AchE, acetylcholinesterase.

RESULTS

In the early enucleate, we refer to cortex immediately surrounding striate cortex as DEC. In the normal animal, cortex on the posterior bank of the lunate sulcus is known to be area V2. After early enucleation, when large shifts have occurred in the location of the striate border, the identity of cortex in the posterior bank can only be inferred by its anatomical location. Nevertheless, to avoid awkward terminology, we shall refer to this region as area V2. Extrastriate cortex in the enucleate refers collectively to DEC and area V2.

CO labeling

CO activity in the striate cortex of the normal neonate shows an immature laminar distribution. CO activity clearly distinguishes layers 6, 4C, and 2/3. CO activity in the neonate is characterised by a clear band that is largely located in layer 4C (Horton, 1984; Kennedy et al., 1985; Spatz et al., 1993). In the enucleate, the laminar distribution of CO in striate cortex is similar to that in the normal neonate (Fig. 2). One minor difference is that although some CO activity is usually detectable in layer 4A of the normal neonate, it was either absent or very weak after both early and late enucleation (Fig. 2).

After enucleation, the distribution of CO activity in layers 4, 5, and 6 in area V2 was normal. The laminar distribution of CO in layers 4, 5, and 6 in DEC was similar to that of area V2. In the normal neonate, CO stripes in area

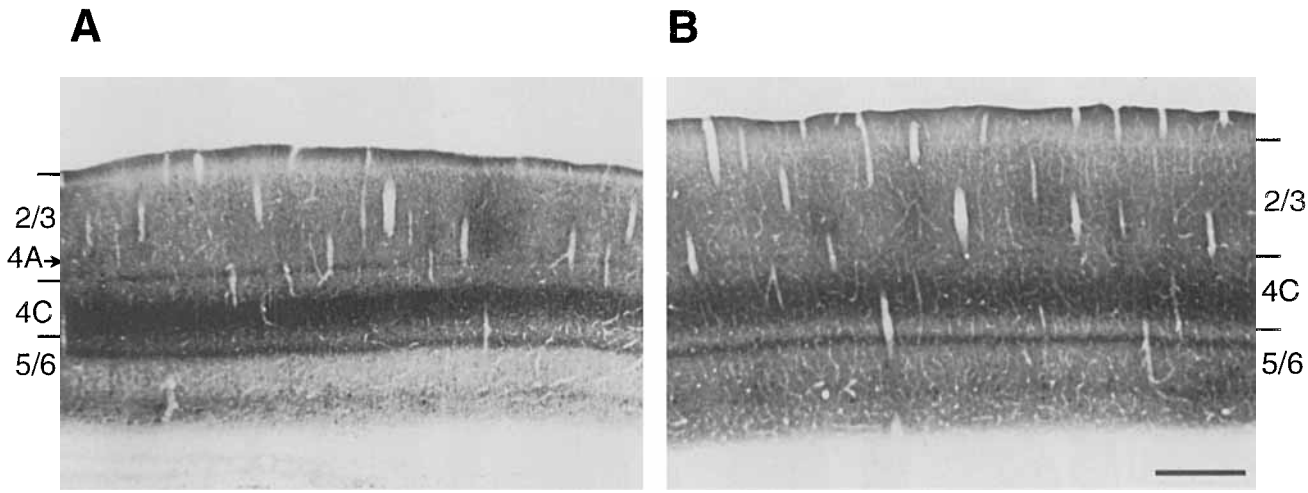

Fig. 2. Cytochrome oxidase (CO) activity distribution in striate cortex in the normal (**A**) and early enucleate BB46 (**B**). The laminar distribution of CO in the normal neonate is similar to that found in the adult, except that there is a cleft at the bottom of layer 4C and the top of layer 5. Following early enucleation, the distribution is similar to that in the normal animal, except for an absence of label in layer 4A. Scale bar = 0.5 mm.

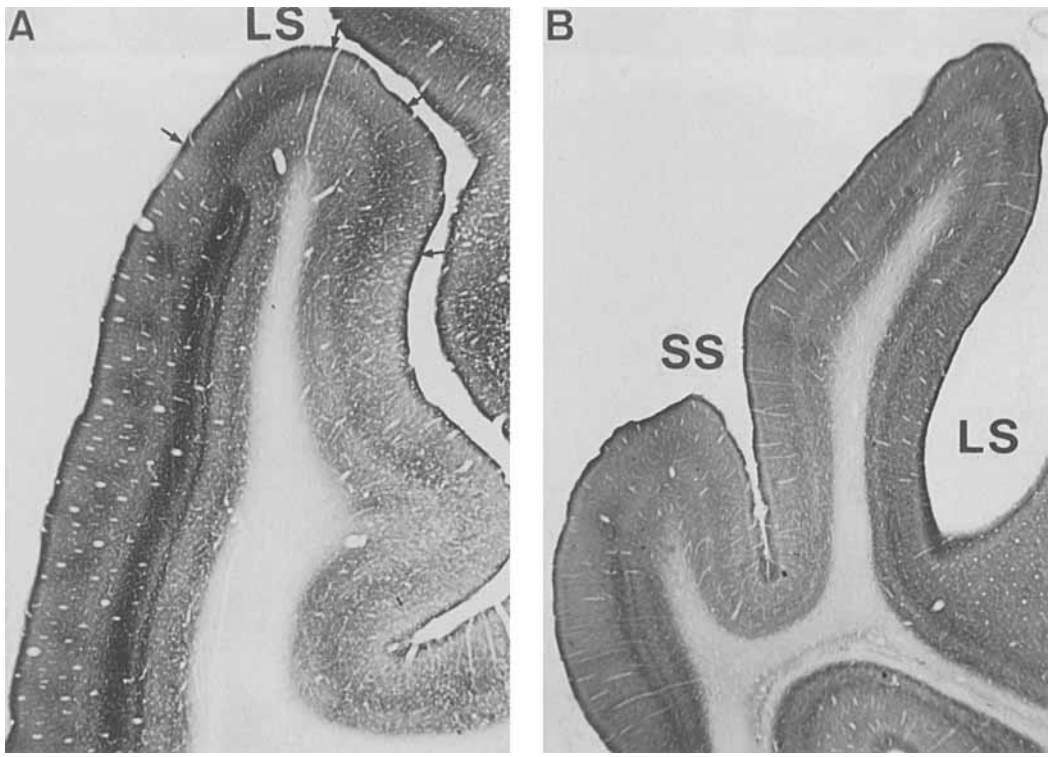

Fig. 3. Cytochrome oxidase (CO) labeling of striate and peristriate cortex in the normal (**A**) and early enucleate BB21 (**B**). In the normal neonate, cytochrome oxidase shows only a very weak stripe pattern in area V2 (indicated by arrows). In the neonate, which received an early enucleation, CO over much of the peristriate cortex on the operculum showed a continuous distribution. We could not detect even weak bands of CO in area V2 on the posterior bank of the lunate sulcus. LS, lunate sulcus; SS, supplementary sulcus. Scale bars = 1 mm.

V2 are present but are weaker than in the adult (Dehay et al., 1986). CO stripes could not be reliably identified in area V2 of the enucleate (Fig. 3).

The disruption of the border of striate cortex after early enucleation leads to an interdigitation of striate and extrastriate cortex that can be seen in Nissl-stained sections. On either side of the border in regions of interdigitation, CO activity was distributed according to an appropriate striate and extrastriate fashion so that the striate border in these regions is no less precise than elsewhere. Figure 4A shows such an interdigitation on the operculum of a neonate that has undergone early enucleation. Two short

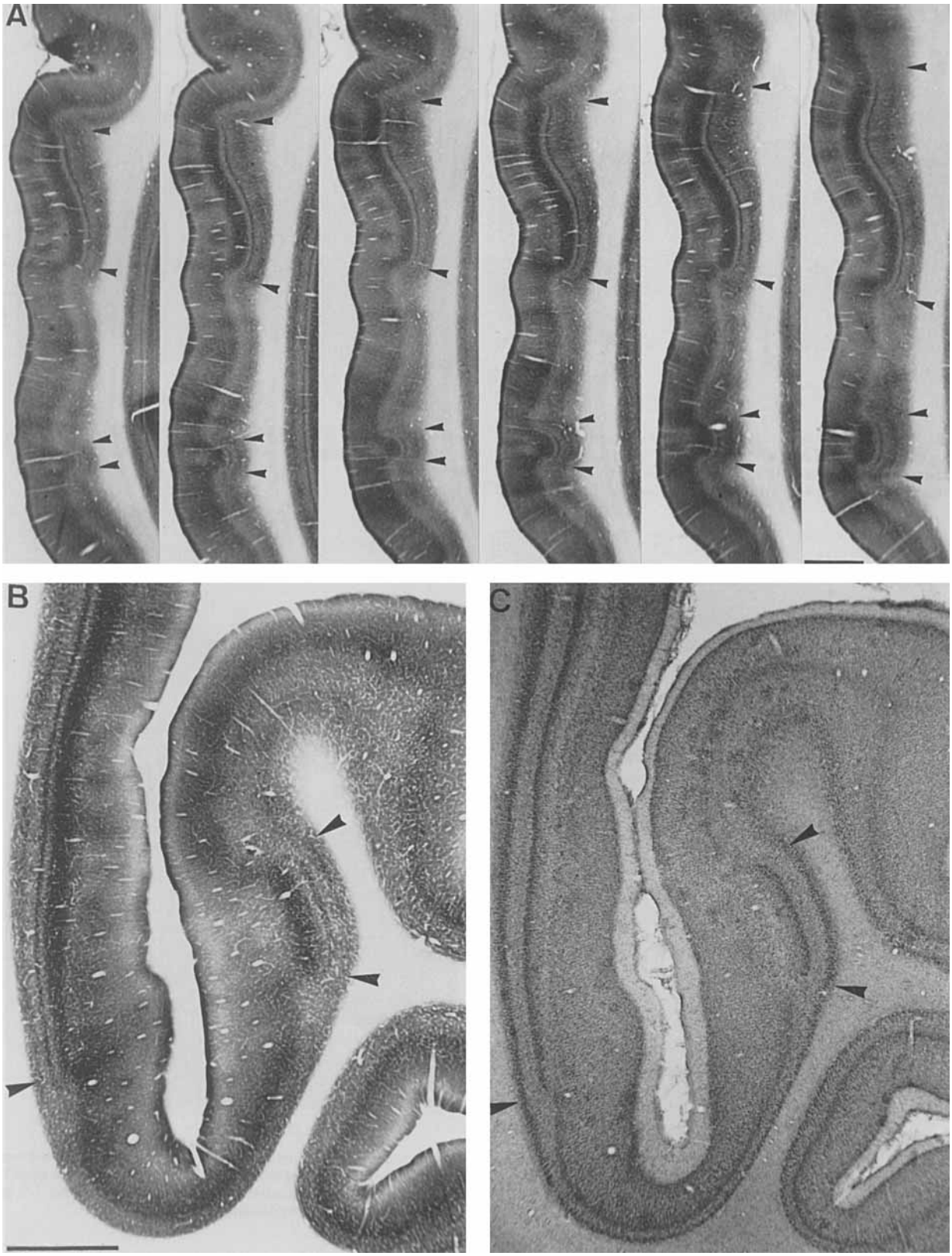

Fig. 4. Cytochrome oxidase (CO) activity distribution in regions where the striate border is perturbed (BB28). The pattern of CO activity in striate cortex is not disturbed by enucleation. This is also true in regions of severe interdigitation at the border as shown in this figure. **A:** Interdigitation of striate cortex on the operculum of a neonate that had undergone enucleation at E68. Even when striate cortex is narrowed down to a thin sliver protruding into extrastriate cortex, it maintains a laminar distribution that is virtually indistinguishable from that found in the normal neonate. **B:** Interdigitation of cortex was also found in the calcarine sulcus. **C:** The adjacent section stained for Nissl shown to illustrate the precise alignment of borders revealed by the two histologic procedures. Arrowheads A–C: limits of striate cortex. Scale bars = 1.5 mm.

stretches of striate cortex, a ventral stretch measuring less than 1 mm across and a dorsal stretch measuring 3–4 mm, can be seen. These protrusions of striate cortex join at more medial levels. Progressing medial to lateral (right to left in the figure), both pieces of striate cortex became narrower before the ventral-most stretch disappears. The characteristic cleft at the base of layer 4C in striate cortex is present in both protrusions. In the smaller protrusion, the cleft is present when the protrusion measures only several hundred microns across. The CO blobs in layers 2/3 are likewise conserved in these narrow stretches of striate cortex. When adjacent CO and Nissl-stained sections were compared, they revealed a perfect match between the areal borders. This is illustrated in Figure 4B from an area 17 indentation in the internal calcarine of an early enucleate.

In medial sections, parts of DEC of the early enucleate show periodic distributions of high CO activity spanning the full cortical width (Fig. 5). In these CO dense patches, enzyme activity is high in both supragranular and infragranular layers. Similar high-frequency CO patches were observed in restricted regions of area V2 on the medial sections, where they were much less frequent than they were in DEC. The extrastriate CO dense patches were found on both the operculum and in the internal calcarine.

CO blob separation in striate cortex was measured in the normal control and enucleates. The frequency distribution is shown in Figure 6, and the mean separation values are shown in Table 2. In the normal animal, there was a nonsignificant tendency for CO blob separation on the operculum to be larger than in the calcarine. In the enucleates, mean CO blob separation values were greater in the calcarine than on the operculum. Statistical comparisons of the means (Mann-Whitney U test) show that in the two early enucleates (E68 and E59), the smaller mean separation on the operculum is significantly different ($P < 0.0001$) from the values on the operculum of the normal and late enucleates (E91, E110). Although comparison between animals is of limited significance due to variations of tissue shrinkage, it shows that calcarine separation values in the enucleates are not significantly different from those in the normal control except for the E110 enucleate, in which mean blob separation was slightly larger ($P < 0.008$). Together, these results suggest that early enucleation leads to a reduction of CO blob separation on the operculum but not in the calcarine.

CO dense patches in extrastriate cortex were detected in both the E59 and E68 enucleated neonates. Mean CO dense patch separation values in the DEC on the operculum were 780 μm (BB28) and 640 μm (BB46) and were significantly larger than the CO blob mean separations of 480 and 520 μm in striate cortex of the same animals ($P < 0.005$). There were no significant differences between the separation values of CO dense patches in DEC in the calcarine and on the operculum. CO dense patches in area V2 in the animal enucleated on E68 were not very numerous and had a mean separation value of 820 μm, which was not significantly different from separation values in the DEC.

AChE labeling

In the neonate, AChE bands appear as dense fiber staining in layer 4 and the bottom of layer 3 (Fig. 7). AChE bands can be detected around E122 and by E133 have become a conspicuous feature of the immature area V2 (Fig. 8). At E122, AChE fibers form a dense plexus centered in layer 4 with only a modest decrease in density between the bands. There is virtually always a band of AChE fibers in area V2 immediately adjacent to the border with striate cortex. The AChE fibers in area V2 show a sharp restriction to this area in the border region (see Figs. 7, 8). The AChE bands can be shown to run perpendicular to the border of striate cortex by sectioning the cortex parallel to the surface (Barone et al., 1994a). In parasaggital sections, small shifts in the position of the bands reflect their perpendicular orientation with respect to the striate border (Figs. 7, 8).

The fetal development of AChE was greatly modified by early enucleation. In a E137 fetus enucleated at E62, there was a dense staining of numerous AChE-positive fibers throughout extrastriate cortex including DEC. The laminar distribution of AChE-positive fibers in striate cortex in this and all other cases was similar to that in the normal control (Fig. 9). As in the normal animal, AChE fibers showed a sharp restriction in the border region to DEC and did not invade striate cortex. In DEC, a single AChE band could be detected at the border of striate cortex. The orientation of the band was different from normal because it did not change position on sequential sections. This indicates an absence of AChE bands oriented perpendicular to the border in DEC. After early enucleation, area V2 showed high levels of AChE staining in layer 4 and the bottom part of layer 3. However, this labeling was continuous, and again there was no indication of the formation of the bands normally found in fetuses of this age (Fig. 10).

In the early enucleate that was examined at a E137, AChE staining was maintained in striate cortex and DEC in the highly perturbed regions near the border of area 17, as shown in Figure 11. In this instance, a small region of DEC was entirely surrounded by striate cortex. Comparison of the sections processed for AChE with the adjacent sections stained for Nissl substance shows that the AChE distribution respects the border of striate cortex.

After early enucleation, there was a massive downregulation of AChE activity during the last month of pregnancy. In neonates that had undergone early fetal enucleation, there was an absence of AChE activity throughout DEC and area V2. AChE activity was also absent in more anterior extrastriate visual regions such as the anterior bank of the lunate sulcus (Fig. 12A). This contrasted with striate cortex, where there was dense staining in layer 4C. In the nonvisual cortex, the density of AChE staining was comparable in the experimental and control neonates, indicating that the absence of AChE-labeled fibers in DEC and extrastriate cortex was not an artefact (Fig. 12B,C).

In the late enucleate (E81 and later), there was only a modest reduction in the size of area 17 (Dehay et al., 1996), and well-defined AChE bands were present in area V2 (Fig. 13).

DISCUSSION

Bilateral enucleation has only minor effects on the intensity and distribution of CO and AChE activity in striate cortex. This contrasts with extrastriate cortex, where both CO and AChE activity were profoundly modified by early enucleation. After early enucleation, the CO stripes in area V2 could not be detected. Instead, high-frequency CO dense patches were observed in DEC and to a much lesser extent in area V2. These results show that the induced cortical region displays novel phenotypic features. After early enucleation, AChE-positive fibers in the fetus failed to form the

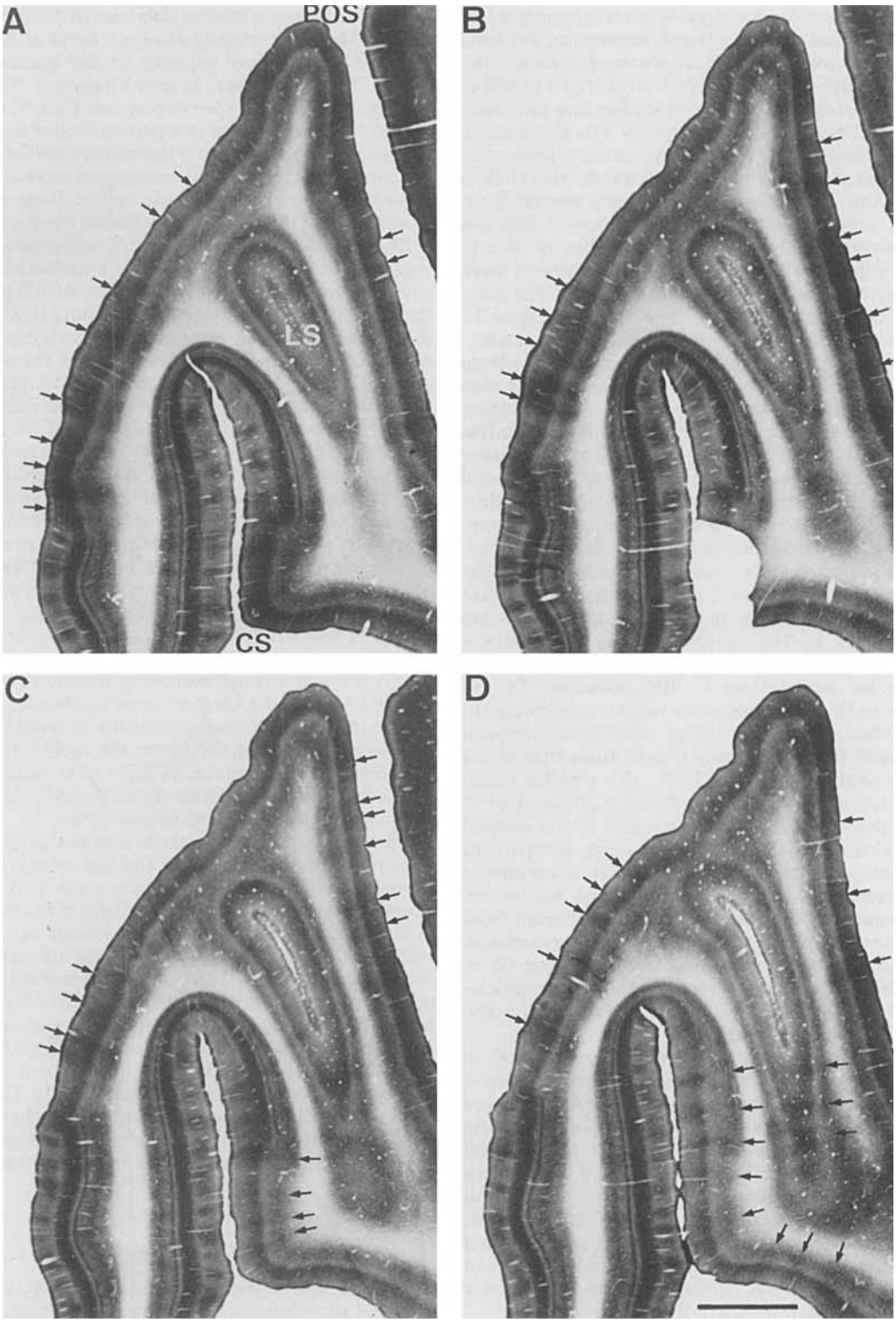

Fig. 5. Cytochrome oxidase (CO) dense patches in default extrastriate cortex (DEC) of a neonate that had undergone early enucleation (BB28). In restricted parts of the DEC, there are periodic fluctuations of CO activity. POS, posterior occipital sulcus; LS, lunate sulcus; CS, calcarine sulcus. Arrows indicate CO blob-like patches. A is lateral and D medial. Scale bar = 2 mm.

thick transient bands that normally run perpendicular to the border of striate cortex. Instead, a dense plexus of fibers was found throughout area V2 and DEC. However, during the last month of gestation, there was a dramatic downregulation of AChE expression in DEC and area V2 of the early enucleate, so that by birth there were virtually no AChE-

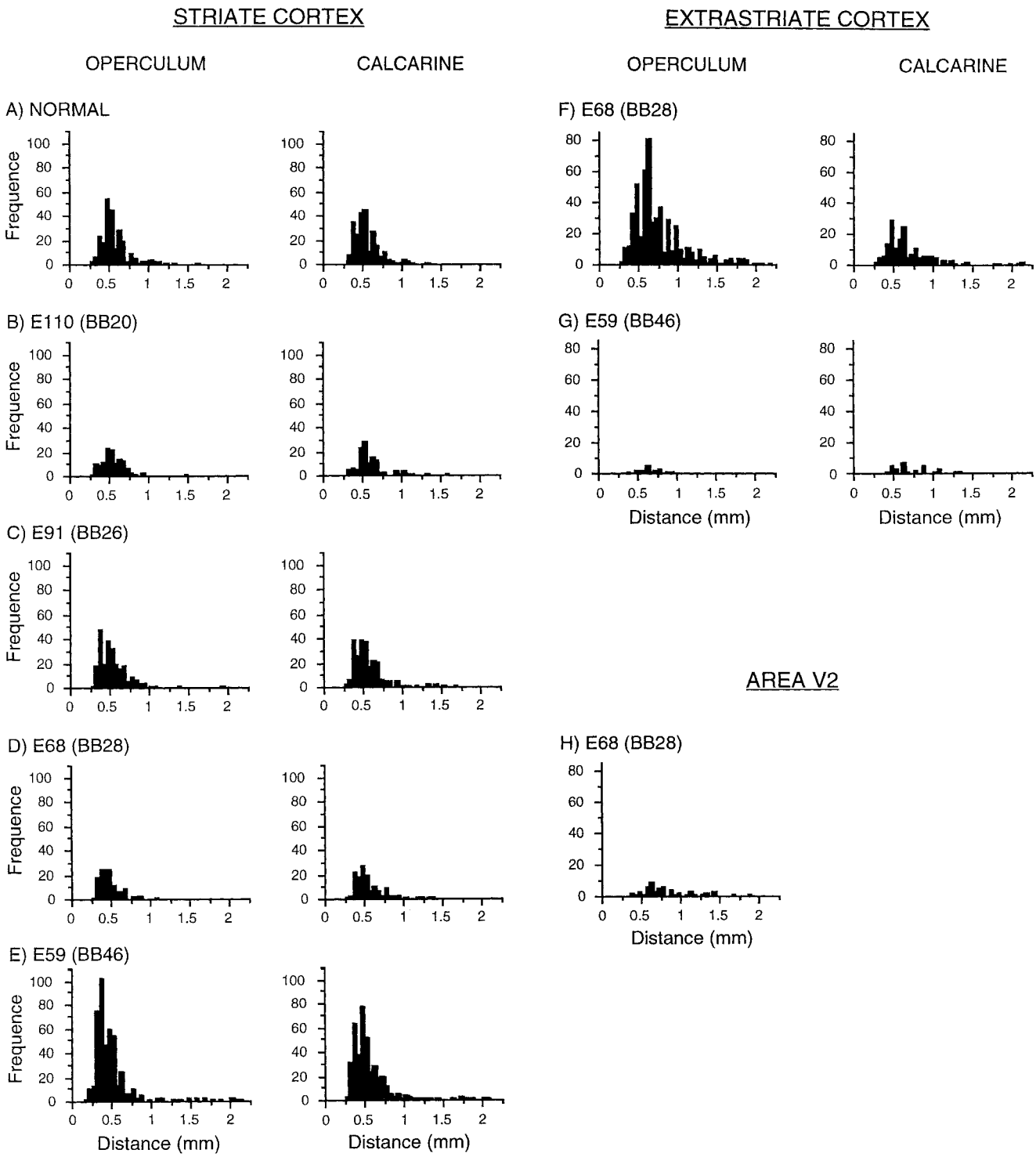

Fig. 6. Histograms showing the distribution of separation values of cytochrome oxidase (CO) blobs in striate cortex and CO dense patches in extrastriate cortex of normal and enucleated neonates.

labeled fibers in extrastriate cortex. These changes in the development of CO and AChE only occurred when there was a substantial shift in the border of striate cortex and therefore were not observed after late enucleation (E81–E110).

Limited influence of enucleation on border formation

Early enucleation leads to a shift in the striate border because there is a reduction of striate cortex accompanied

by the formation of DEC (Rakic, 1988; Dehay et al., 1996). In each early enucleate, we found narrow protrusions of striate cortex into DEC as well as islands of DEC in the striate cortex near the border (Rakic et al., 1991; Dehay et al., 1996). A possible explanation of this ragged border in the early enucleate is that the reduction of the number of lateral geniculate nucleus (LGN) fibers leads to a reduction of cohesion among fibers. This drop in cohesion becomes critical around the perimeter of the striate cortex where the occasional islands of DEC are found. These results suggest that the mechanisms generating the striate border are unable to accommodate totally large shifts in border location (Dehay et al., 1996).

TABLE 2. Mean Cytochrome Oxidase Blob Separation Values (mm)

Case	Age at enucleation	Striate cortex		Default extrastriate cortex		Area V2
		Operculum	Calcarine	Operculum	Calcarine	
Normal		0.57	0.55			
BB20	E110	0.54	0.60			
BB26	E91	0.53	0.56			
BB28	E68	0.48*	0.55	0.78	0.76	0.82
BB46	E59	0.52*	0.69	0.64	0.74	

*Mann Whitney nonparametric test, $P < 0.005$.

The striate cortex in the early enucleate was remarkably normal in terms of the intensity and laminar distribution of CO and AChE activity. This suggests a tight coupling between the developmental mechanisms generating the cytoarchitectonic features of striate cortex and the laminar distribution of CO and AChE activity. The tightness of this coupling in striate cortex is revealed by the appropriate patterns of CO and AChE activity in this area being maintained up to its highly serrated border.

Influence of enucleation on CO blob frequency in striate cortex

In the normal animal, CO blobs form a regular repeating lattice in striate cortex that is directly related to its functional architecture (for review, see Martin 1988). In the normal newborn monkey, there is a regular array of CO blobs in supragranular layers showing that this feature develops independently of visual experience (Horton, 1984; Kennedy et al., 1985; Dehay et al., 1986; Horton and Hocking, 1996). Because the age of the early enucleation is before the generation of the supragranular layers, our results (Dehay et al., 1989; Kennedy et al., 1990; present results) along with those of Kuljis and Rakic (1989) suggest that development of the functional architecture of the

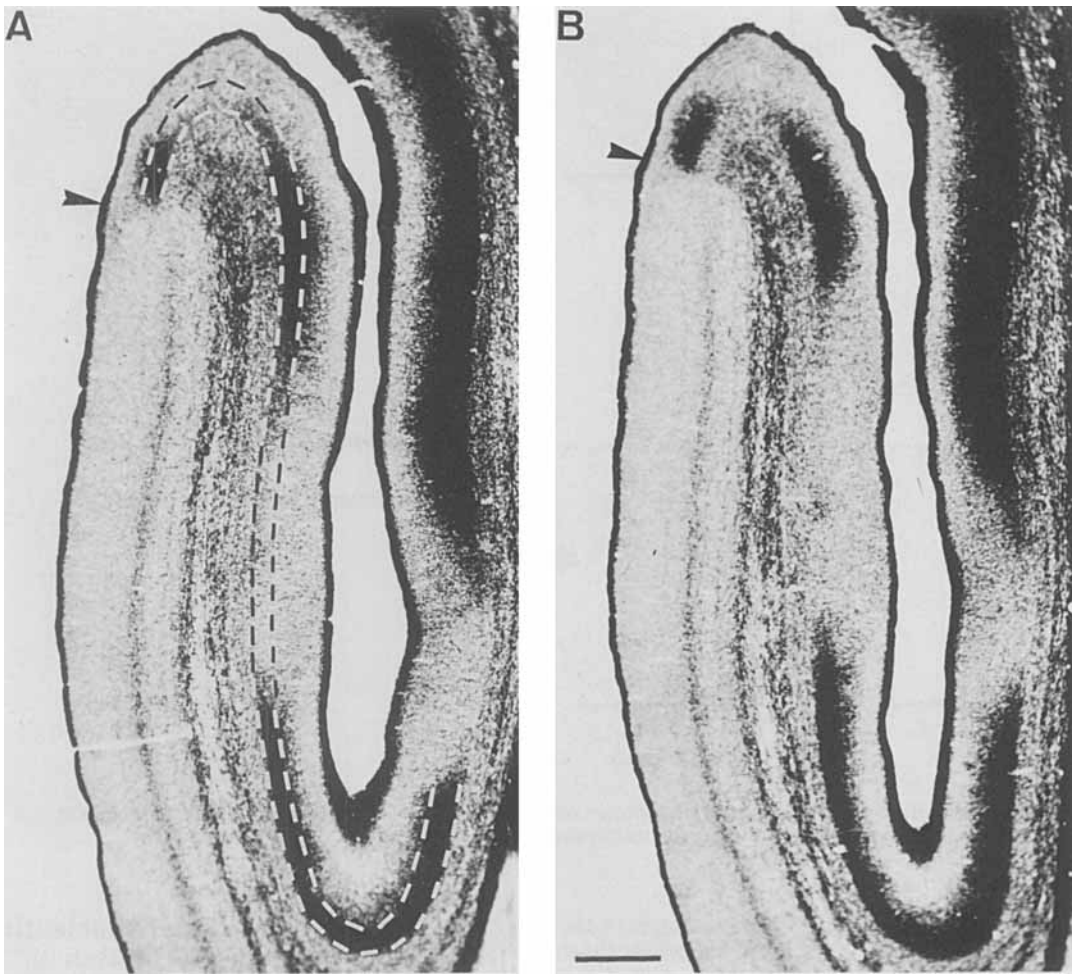

Fig. 7. Acetylcholinesterase activity in striate and extrastriate cortex in the banks of the lunate sulcus of the normal neonate. Dotted lines in A indicate the limits of layer 4 in area V2 on the posterior bank of the lunate sulcus. Section separation, 0.540 mm. Arrowheads indicate area 17 border. Scale bar = 1 mm.

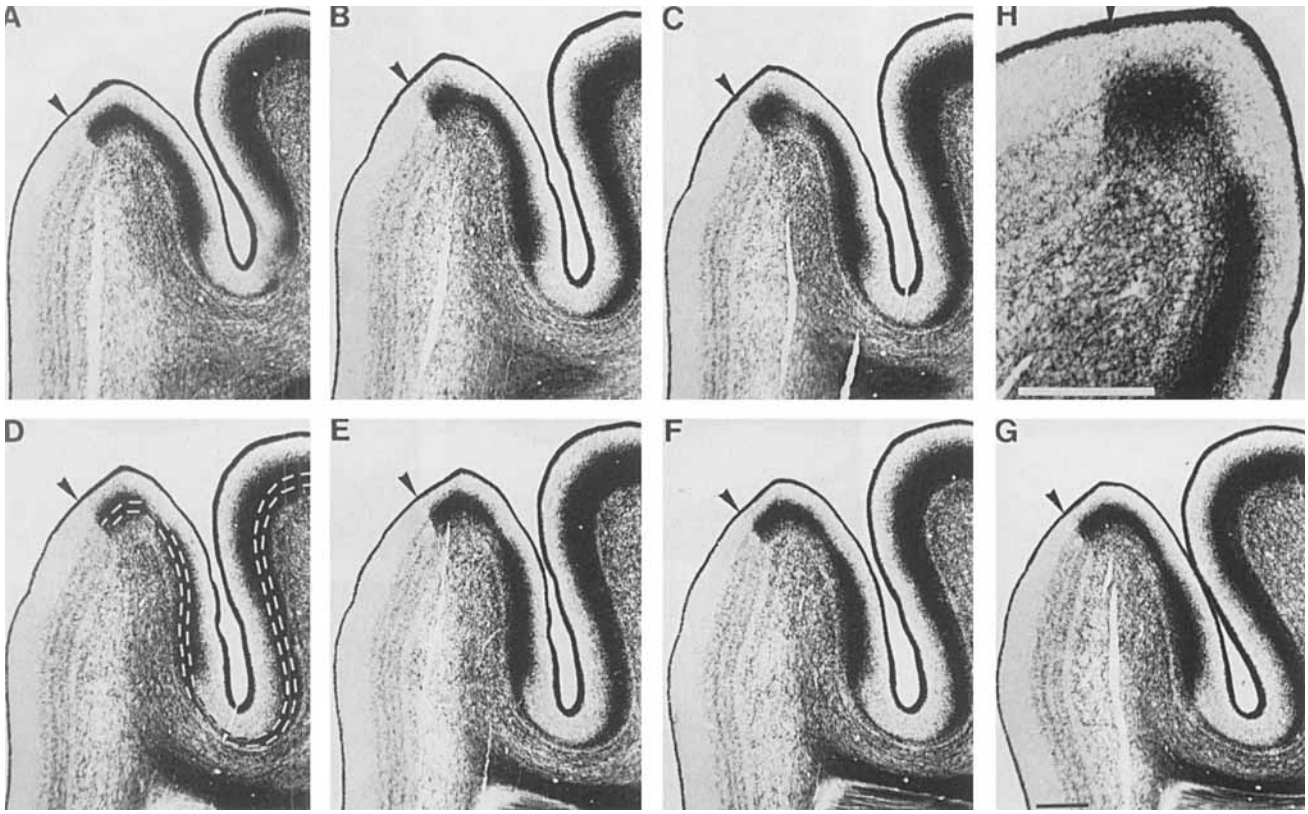

Fig. 8. Acetylcholinesterase activity in striate cortex and extrastriate cortex in the banks of the lunate sulcus of the normal E122 fetus. A is lateral and G medial. Section separation, 0.180 mm. Dotted lines in D indicate the position of layer 4 in area V2 in the posterior bank of the lunate sulcus. Arrowheads indicate position of the border of area 17. Scale bar = 1 mm in A–G, 1 mm in H.

striate cortex, as reflected by CO blob formation, occurs independently of ascending retinal activity. Because the overall blob frequency is similar in early enucleates and normals and given that there is a 70% reduction in the dimensions of the striate cortex, we can deduce that early enucleation leads to an important reduction in the number of CO blobs in striate cortex.

In the normal animal, we found that the mean separation values for CO blobs in the calcarine were slightly lower than on the operculum, confirming previous findings (Livingstone and Hubel, 1984). This contrasts with the early enucleate, in which mean CO blob separation on the operculum was significantly smaller than in the calcarine.

The abnormally low mean separation values of CO blobs in striate cortex on the operculum of the enucleate could be related to the much larger reduction of striate cortex on the operculum compared with that in the calcarine fissure. One possibility is that the greater susceptibility of blob separation and areal reduction on the operculum are developmentally linked to differences in the central magnification of foveal and peripheral representations in the ascending pathways (Dehay et al., 1996).

CO labeling in DEC and area V2

In the normal neonate, CO bands are present in area V2, showing that they develop independently of visual input (Dehay et al., 1986; Dehay and Kennedy, 1988; Horton and Hocking, 1996). After early enucleation, CO bands fail to develop in area V2. However, CO bands are difficult to detect in neonatal area V2; therefore, their absence in the enucleate could result merely from a reduction in their intensity.

The high-frequency CO dense patches in DEC (and to a much lesser extent in area V2) are characteristic of the early enucleate. The CO dense patches showed a mean center-to-center spacing of 760-780 μm. This is much smaller than the 2-mm separation values of CO bands in area V2 (Barone et al., 1996) and significantly larger than the striate CO blobs in the same animals (480–520 μm). Although the sample size in area V2 was small, separation values were not significantly different from that in DEC.

The extrastriate CO dense patches are largely restricted to DEC. Therefore, they are found in a cortical region that was originally destined to become striate cortex and that, late in development, had acquired area 18 cytoarchitectonics. Superficially at least, the CO dense patches are more similar to CO blobs in striate cortex than to CO stripes in area V2, although they might well be unrelated to either (see section on Implications for theories of cortical specification, below).

AChE labeling in DEC and area V2

AChE activity is dense in area V2 throughout prenatal and early postnatal development in the normal animal (Barone et al., 1994a). After early enucleation, AChE fibers are present in extrastriate cortex during early prenatal development. Although AChE fibers in area V2 in the early

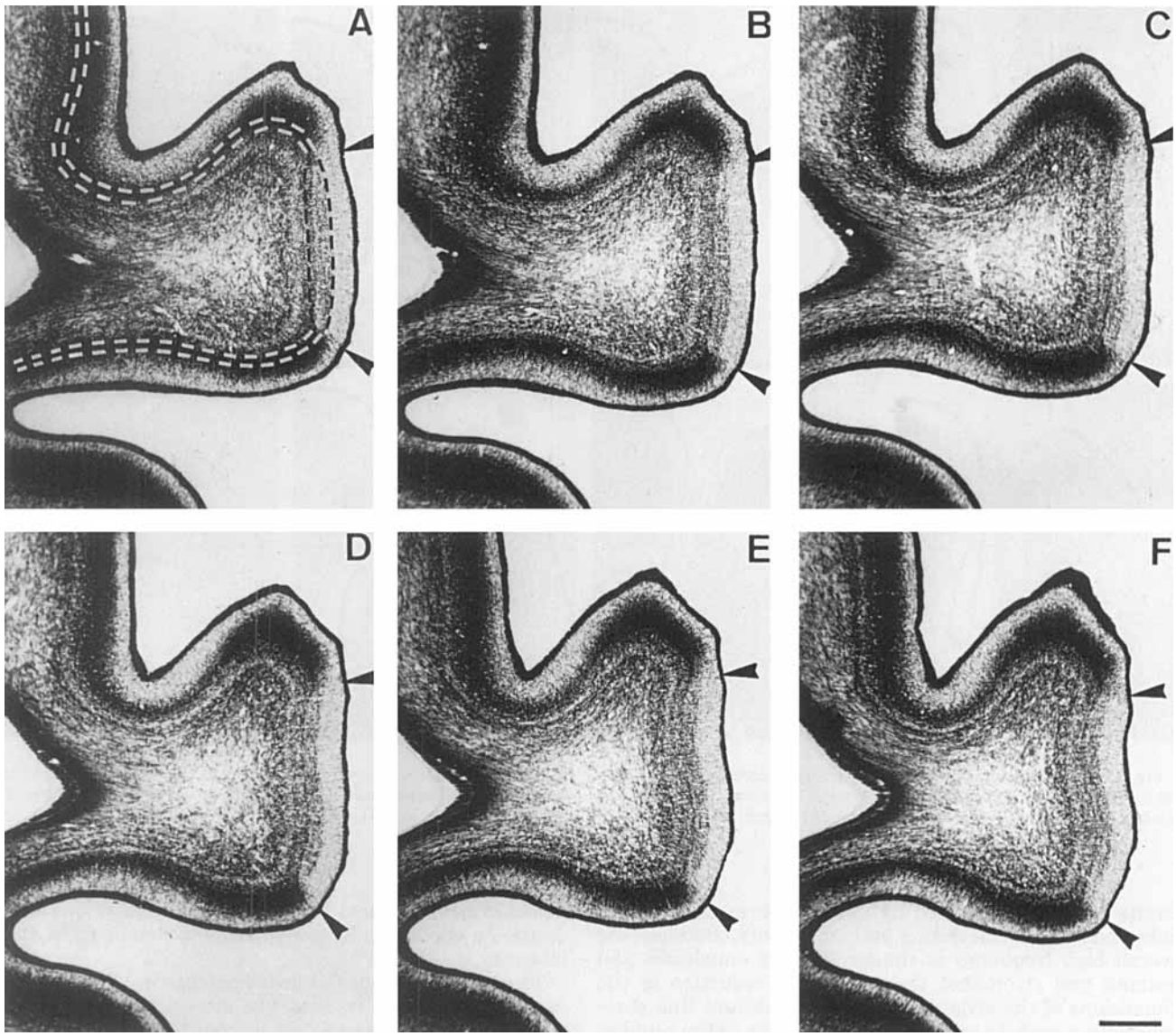

Fig. 9. Acetylcholinesterase (AChE) activity in default extrastriate cortex (DEC) in the E137 fetus previously enucleated at E62 (BB104). In the early enucleate, the striate cortex, adjacent to a supplementary sulcus, occupies only a small fraction of the operculum and is located far posterior to the lunate sulcus (not shown in this microphotograph). Immediately adjacent to the reduced striate cortex, and running along much of its length, there is a single band of AChE fibers invading layer 3. This band does not appear to run orthogonal to the border as is the case in the normal. Section separation: 0.120 mm. Dotted lines in A indicate the position of layer 4 in DEC and area 17. Arrowheads indicate the position of the border of area 17. A is lateral and F medial. Scale bar = 1 mm.

enucleate have the appropriate laminar distribution, enucleation in some way prevents band formation, both in DEC and in area V2. During the last month of gestation of the enucleates, there is a rapid depletion of AChE activity, so that by birth the entire visual cortex outside area 17 is largely devoid of AChE-positive fibers.

To understand the present findings better, we need to consider the origin of the fibers expressing AChE and their developmental significance in the immature cortex.

In a number of species, a transient neocortical expression of AChE has been related to thalamic fiber input and shown not to be due to cholinergic forebrain projections (Robertson et al., 1985, 1988, 1991; De Carlos et al., 1995; see Hanes et al., 1992 for review). Hence, the transient AChE bands in monkey area V2 might correspond to a developmental stage of the banded pulvinar input to this area (Curcio and Harting, 1978). However, this is unlikely given that the pulvinar projection to area V2 overlaps the thin and thick CO bands (Livingstone and Hubel, 1982; Levitt et al., 1995). This contrasts with the AChE bands that are uniquely centered on the CO thin bands (Barone et al., 1996).

The failure to form AChE bands suggests that the AChE-positive fibers in the bands originate from a structure that is profoundly modified by the early enucleation. There are two candidate structures: the LGN and striate cortex (Dehay et al., 1996). The LGN provides only a weak input to area V2 in monkeys (Bullier and Kennedy, 1983), and it is difficult to conceive that the few intercalated LGN neurons involved in this projection set up such a conspicuous feature

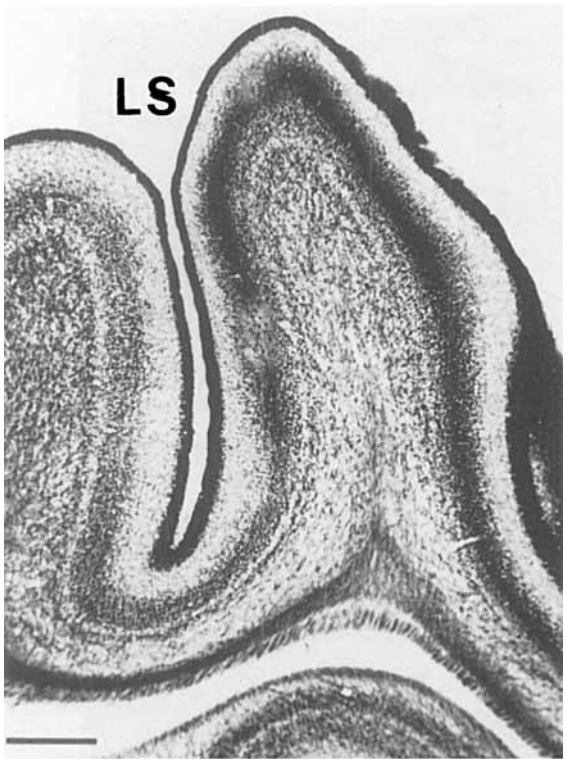

Fig. 10. Acetylcholinesterase activity on the operculum and in presumptive area V2 in the posterior bank of the lunate sulcus in the E137 fetus previously enucleated at E62 (BB104). No indication of acetylcholinesterase bands can be seen in area V2. LS: lunate sulcus. Scale bar = 1 mm.

as the AChE bands. In contrast, the striate cortex provides a major input to area V2. This input is to layer 4 and the supragranular layers (Zeki, 1969, 1975; Wong-Riley, 1978; Rockland and Pandya, 1979; Lund et al., 1981; Weller and Kaas, 1983; Van Essen et al., 1986), layers in which the AChE-positive fibers are located (Barone et al., 1994a). It has been suggested that striate cortical projections can be AChE positive (Fitzpatrick and Diamond, 1980). If the AChE fibers originate from the striate cortex, then we can speculate that they issue from the CO blobs (Livingstone and Hubel, 1984). If this is the case, then the 70% reduction of striate cortex could deplete this projection to a level that is insufficient to maintain band formation. Further, because both DEC and area V2 are occupied by the AChE-positive fibers, the large expansion of the target of striate cortex might also contribute to the loss of the band pattern.

The significance of the transient AChE expression in the cortex is not clear. AChE is not restricted to cholinergic systems, suggesting alternative functions to that of the hydrolysis of acetylcholine (Greenfield, 1984). Recent evidence shows that some forms of AChE act as proteases and could therefore regulate cell growth and development (Small, 1990; however, see Ling et al., 1995). Hence, surface-bound or diffusible AChE could be involved in axon growth

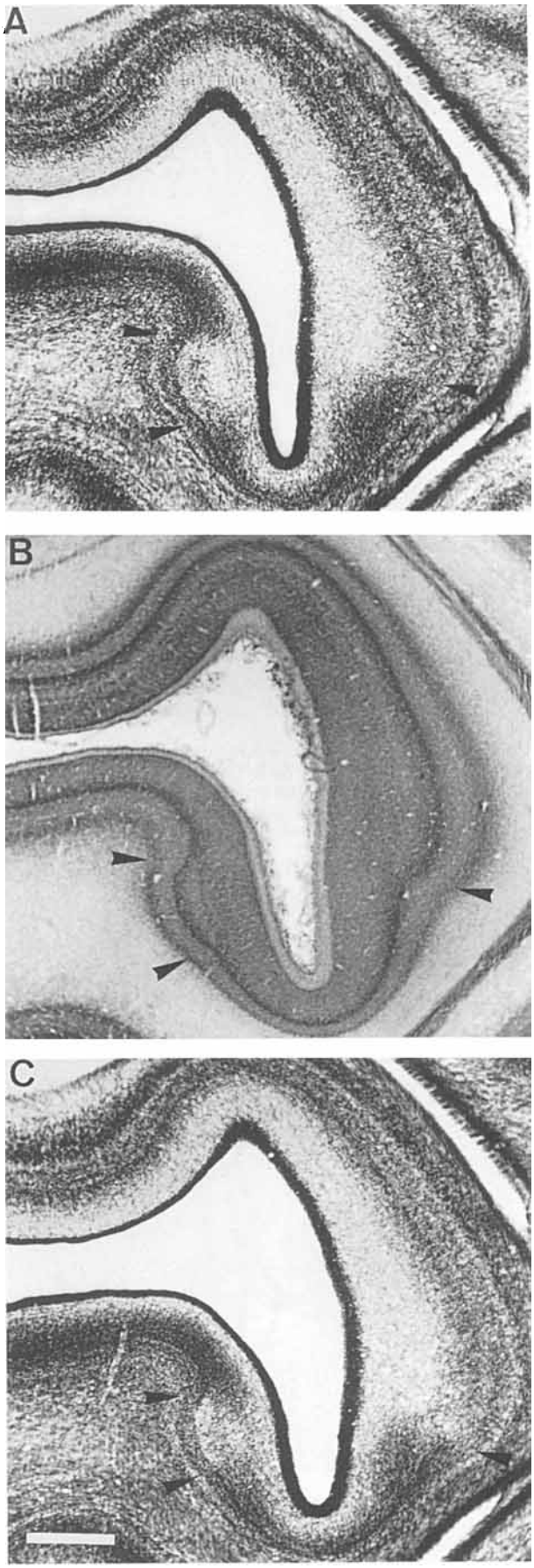

Fig. 11. Island of default striate cortex in the internal calcarine of the E137 fetus that had undergone early enucleation (BB104). **A,C:** Acetylcholinesterase-reacted sections. **B:** Nissl-stained section. Arrowheads in A–C: limits of striate cortex. Scale bar = 1 mm.

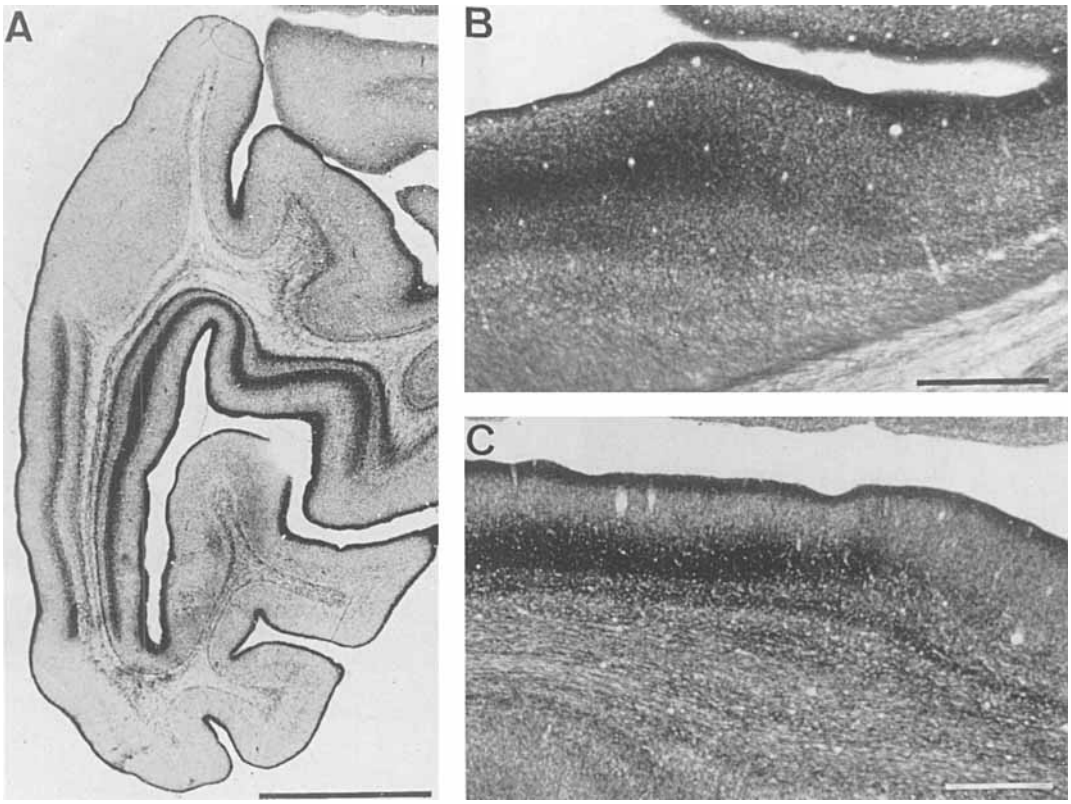

Fig. 12. Acetylcholinesterase activity in striate, default extrastriate cortex, and extrastriate cortex. **A:** In the neonate that had undergone early enucleation (BB46). Enzyme levels in cortical regions anterior to the visual cortex were similar in this enucleate and normal controls as can be seen by comparing the auditory cortex in **B** (the early enucleate, BB46). **C:** Normal control. This figure reveals the extensive downregulation of acetylcholinesterase activity during the last month of gestation following early enucleation. Scale bars = 5 mm in A, 1 mm in B,C.

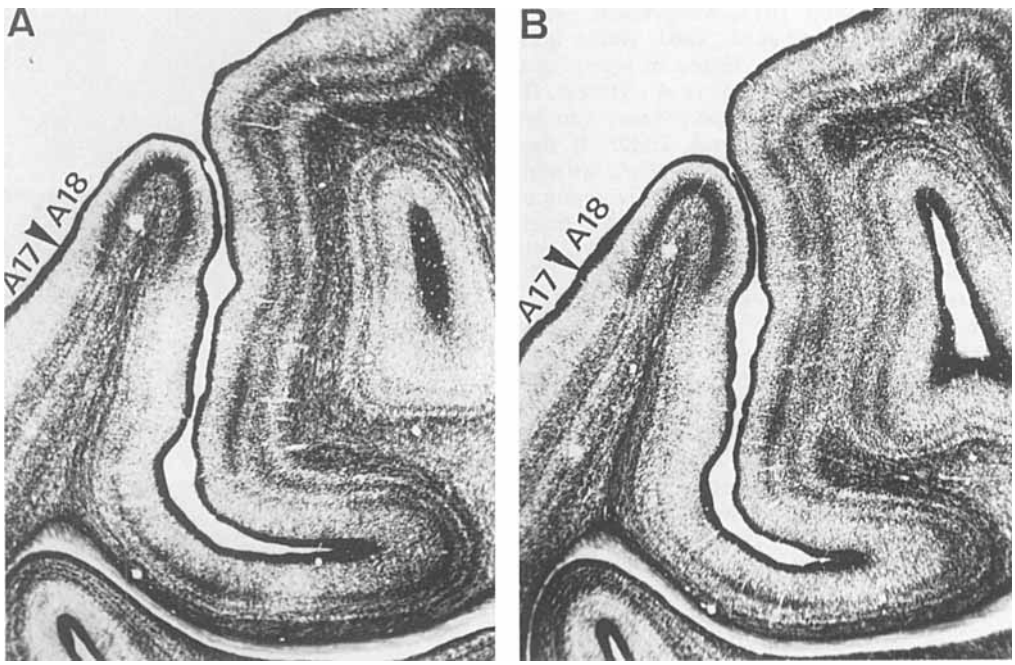

Fig. 13. Acetylcholine activity in striate and extrastriate cortex of a late enucleate (BB35). Arrowheads: limits of striate cortex. Scale bar = 2 mm.

through the extracellular matrix and might, therefore, be related to late stages of axonal growth and motility (Layer et al., 1993). The fact that the AChE fibers disappear in the last month of gestation of the enucleate is unlikely to be the consequence of cell loss or axon elimination. The most probable explanation is that the fibers persist but cease to express AChE. If this is the case, early enucleation (perhaps because of the suppression of ascending neural activity) might lead to changes in the final stages of axon mobility in well-defined subregions of area V2 and DEC.

Implications for theories of cortical specification

It has been suggested that cortex that was destined to become striate cortex and that, after enucleation, fails to acquire the appropriate cytoarchitecture constitutes a novel cortical area—area X (Rakic, 1988). This author suggested that area X is a hybrid cortex combining both striate and extrastriate features. It was hypothesised that the hybrid cortex contained neurons that were genetically programmed to be part of striate cortex and yet had accommodated input characteristic of area V2. This suggestion is in line with studies showing, on the one hand, that there is a fate map of neocortical areas in the ventricular zone (Barbe and Levitt 1991; Arimatsu et al., 1992; Dehay et al., 1993; Cohen-Tannoudji et al., 1994; Soriano et al., 1995) and, on the other hand, that cortical development is strongly influenced by peripheral inputs (Van der Loos and Woolsey, 1973; Rakic, 1988; Dehay et al., 1989, 1996; O'Leary, 1989; Killackey, 1990).

Thus, it was speculated that the mismatch between the early genetic specification (in the form of an early ventricular fate map of striate cortex) and the late afferent specification (response to input appropriate to area V2) induces a cortical area combining phenotypic features of the two areas.

In our previous reports, we have used neither the term hybrid cortex nor area X to designate the expanded extrastriate cortex after enucleation. This was because we found that the additional extrastriate region (i.e., DEC) displayed no striate cortex features, was indistinguishable from normal extrastriate cortex, and consequentially possessed no combination of features justifying the term hybrid (Dehay et al., 1996). In the present study, we continue to use the term DEC because, as we argue below, neither the CO nor the AChE labeling conclusively shows hybrid features.

In the present study we show that DEC has CO dense patches. What is the status of these DEC CO dense patches with respect to CO modulation in normal visual cortex? Given their presence in DEC, we first need to consider whether there are any grounds to consider them equivalent to CO blobs in striate cortex.

One possibility is that CO dense patch formation in DEC is triggered by thalamic afferents (Fig. 14). In the normal animal, CO blobs in striate cortex receive input from the koniocellular (K) pathway of the LGN (Weber et al., 1983; Hendry and Yoshioka, 1994). The K cells are thought to constitute a third visual pathway going from the LGN to striate cortex in addition to the parvocellular and magnocellular streams (Casagrande, 1994; Hendry and Yoshioka, 1994).

The K pathway could be a good candidate for the specification of CO dense patches in DEC (Fig. 14A). Because K cells in the LGN receive their major input from the superior colliculus (Lachica and Casagrande, 1993; Harting et al., 1991; Feig and Harting, 1994), one would expect the K pathway to be less susceptible to deafferentation from the retina; this might explain the presence of the CO dense patches in DEC. In line with this hypothesis of a thalamic specification of CO dense patches in DEC blobs is that injections of retrograde tracers in the superficial layers of the DEC of early enucleates leads to labeled neurons in the reduced LGN (unpublished finding). If these labeled neurons in the LGN were part of the K pathway, which in the normal animal projects to striate cortex (and which is distinct from those interlaminar cells that project to extrastriate cortex (S. Hendry, personal communication), then these cells could trigger the formation of the CO dense patches in DEC. According to this scheme, the parvocellular and magnocellular streams determine the dimensions of striate cortex, whereas the K pathway plays a role in

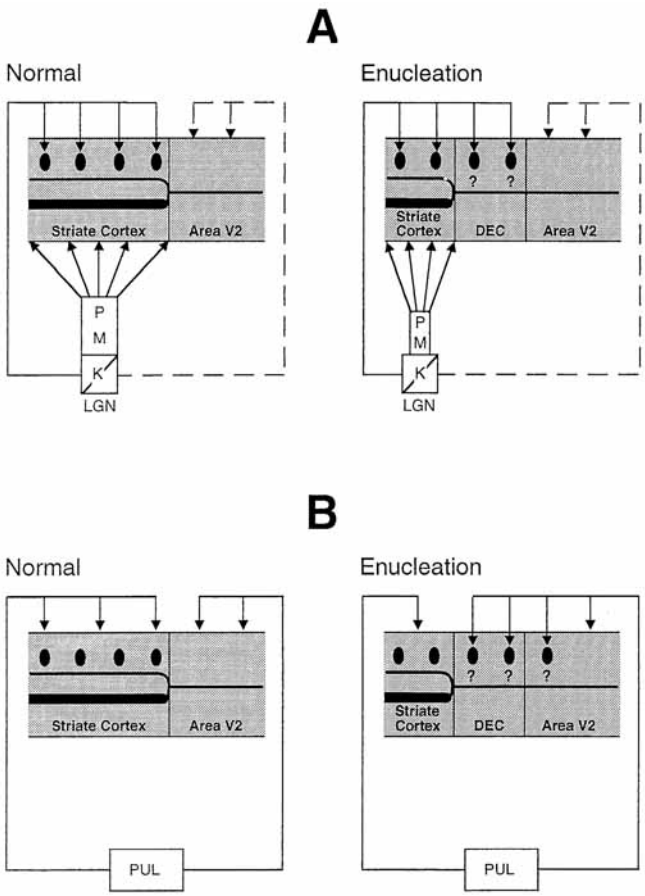

Fig. 14. Hypothetical mechanisms of afferent specification of monkey visual cortex. Deafferentation of the visual cortex, subsequent to enucleation, leads to a reduction of striate cortex, showing that thalamic projections play an important role in determining the area dimensions of the striate cortex. Thalamic input could also be involved in the development of cytochrome oxidase (CO) dense patches in default extrastriate cortex (DEC). **A:** One possibility is that the K projection to the superficial layers of striate cortex is involved in the development of CO blobs in striate cortex. According to this hypothesis, CO dense patches in DEC cortex could be triggered by the projection from the K compartment of the reduced lateral geniculate nucleus to the upper layers of this region, because the K pathway may possibly be spared by the enucleation, due to the input of superior colliculus to these layers. **B:** In the normal animal, pulvinar input to the upper layers of area V2 could be involved in the development of thick and thin stripes. According to this hypothesis, DEC could accommodate this pulvinar input, and this input could trigger CO patch formation. For references, see text. P, parvocellular; M, magnocellular; K, Koniocellular; LGN, lateral geniculate nucleus; PUL, pulvinar.

specifying the CO blobs and therefore the periodicity of the functional architecture. This would make the CO dense patches in DEC truly equivalent to the striate CO blobs of the normal animal.

The above considerations show that DEC could be a hybrid in so far as it exhibits a combination of striate and extrastriate features. However, in the above scenario, the hybrid nature of this cortex is uniquely created by afferent specification. An alternative possibility is that the CO dense patches in the DEC field develop independently of thalamic input and are the consequence of an early specification at the level of the ventricular zone. Therefore, they would reflect the early striate identity of this cortical region. According to this theory, CO blob formation would be an intrinsic feature of the striate cortical field.

However, we have to guard against making the mistake of assuming that there are only two sorts of solutions to the problem of the development of CO dense patches in DEC. In fact, we cannot be sure that the CO dense patches in DEC are in any way equivalent to striate CO blobs. Their periodicity alone being 23–41% wider than the striate CO blobs throws some doubt on the probability of there equivalence. Livingstone and Hubel (1982) suggested that high CO activity reflects thalamic input, and one possibility is that the periodic CO activity in the DEC reflects pulvinar input to this structure (Fig. 14B). This would fit with the correspondence of the CO dense patches in DEC with the periodicity of pulvinar input to striate cortex (Ogren and Hendrickson, 1977) as well as the presence of high-frequency CO patches in area V2. According to this theory, pulvinar input, which in the normal animal is thought to project to the thick and thin stripes of area V2 (Levitt et al., 1995), would be setting up a unique set of CO fluctuations in DEC and to a lesser extent in area V2. In this case, the CO dense patches in DEC would have no kinship to striate cortex blobs but would have more in common with area V2 stripes.

In the absence of an understanding of the precise nature of the thalamic input to the DEC, we conclude that we cannot distinguish between these developmental scenarios. Therefore, we have decided to use the term DEC and not hybrid cortex in the present study, because the latter makes as yet unverifiable assumptions about the development of this region.

Reductions in the LGN compartments have a profound influence on the development of their primary target, striate cortex. The modified striate cortex will, in turn, influence the development of its principal target, area V2. Hence, differential effects on the parvocellular, magnocellular, and K streams could influence, in a complex fashion, the output of striate cortex to parietal and temporal cortices.

The mechanisms generating the cytoarchitectonics and the histochemistry of extrastriate cortex are uncoupled by early enucleation. The failure of extrastriate cortex to acquire its appropriate AChE labeling suggests that the specification of extrastriate cortex is a late event that is at least partially dependent on afferents from striate cortex. In this way, the massive reduction of striate cortex leads to a deafferentation of extrastriate cortex, which in turn results in a failure of this cortex to acquire its normal AChE phenotype.

CONCLUSIONS

Because early enucleation leads to a reduction in the size of striate cortex, we can conclude that the dimensions of striate cortex are, at least partially, specified by the sensory periphery. In the present study, we show that the DEC displays novel features. These could well be solely the consequences of modified afferent specification, although we cannot exclude the possibility that they reflect an early specification in the ventricular zone of this region.

Except for the reduction in size, early enucleation has little effect on the characteristics of striate cortex. This contrasts with extrastriate cortex, where enucleation has a drastic influence on patterns of both CO and AChE labeling. These results suggest that afferent specification of the cortex acts in a cascade fashion, spreading from a primary area and relaying to more distal regions by cortical pathways. These findings suggest that peripheral damage during development can be expected to trigger widespread modifications of the cerebral cortex. These findings could be important in future studies investigating the consequences of congenital anomalies in peripheral sense organs in human brain development.

ACKNOWLEDGMENTS

The authors thank Vivien Casagrande and Stewart Hendry for their helpful comments on an earlier draft. Funding was provided by E.E.C. Grant SC1 622; Human Frontier Grant RG-55/94B; MRE and a NATO Travel Grant.

LITERATURE CITED

Arimatsu, Y., M. Miyamoto, I. Nihonmatsu, K. Hirata, Y. Uratani, Y. Hatanaka, and K. Takaguchi-Hayashi (1992) Early regional specification for a molecular neuronal phenotype in the rat neocortex. Proc. Natl. Acad. Sci. USA *89:*8879–8883.

Barbe, M.F., and P. Levitt (1991) The early commitment of fetal neurons to the limbic cortex. J. Neurosci. *11:*519–533.

Barone, P., C. Dehay, M. Berland, and H. Kennedy (1994a) Developmental changes in the distribution of acetylcholinesterase in the extrastriate cortex of the monkey. Dev. Brain Res. *77:*290–294.

Barone, P., C. Dehay, M. Berland, and H. Kennedy (1994b) Segregation of functional visual pathway in the prenatal monkey. Soc. Neurosci. Abstr. *20:*215.

Barone, P., C. Dehay, M. Berland, and H. Kennedy (1996) Role of directed growth and target selection in the formation of cortical pathways: Prenatal development of the projection of area V2 to area V4 in the monkey. J. Comp. Neurol. *374:* 1–20.

Blasdel, G.G., and J.S. Lund (1983) Termination of afferent axons in macaque striate cortex. J. Neurosci. *3:*1389–1413.

Bullier, J., and H. Kennedy (1983) Projection of the lateral geniculate nucleus on to cortical area V2 in the macaque monkey. Exp. Brain Res. *53:*168–172.

Casagrande, V.A. (1994) A third parallel visual pathway to primate area V1. Trends Neurosci. *17:*305–310.

Cohen-Tannoudji, M., C. Babinet, and M. Wassef (1994) Early determination of a mouse somatosensory cortex marker. Nature *368:*460–463.

Curcio, C.A., and J.K. Harting (1978) Organization of pulvinar afferents to area 18 in the squirrel monkey: Evidence for stripes. Brain Res. *143:*155–161.

DeCarlos, J.A., B.L. Schlaggar, and D.D.M. O'Leary (1995) Development of acetylcholinesterase-positive thalamic and basal forebrain afferents to rat embryonic rat neocortex. Exp. Brain Res. *104:*358–401.

Dehay, C., and H. Kennedy (1988) The maturational status of thalamocortical and callosal connections of visual areas V1 and V2 in the newborn monkey. Behav. Brain Res. *29:*237–244.

Dehay, C., H. Kennedy, and J. Bullier (1986) Callosal connectivity of visual areas V1 and V2 in the newborn monkey. J. Comp. Neurol. *254:*20–33.

Dehay, C., G. Horsburgh, M. Berland, H.P. Killackey, and H. Kennedy (1989) Maturation and connectivity of the visual cortex in monkey is altered by prenatal removal of retinal input. Nature *337:*265–267.

Dehay, C., G. Horsburgh, M. Berland, H.P. Killackey, and H. Kennedy (1991) The effects of bilateral enucleation in the primate fetus on the parcellation of visual cortex. Dev. Brain Res. *62:*137–141.

Dehay, C., P. Giroud, M. Berland, and H. Kennedy (1993) Modulation of the cell cycle contributes to the parcellation of the primate visual cortex. Nature *366:*464–466.

Dehay, C., P. Giroud, M. Berland, H.P. Killackey, and H. Kennedy (1996) The contribution of thalamic input to the specification of cytoarchitectonic cortical fields in the primate: effects of bilateral enucleation in the fetal monkey on the boundaries, dimensions and gyrification of striate and extrastriate cortex. J. Comp. Neurol. *367:*70–89.

DeYoe, E.A., and D.C. Van Essen (1985) Segregation of efferent connections and receptive field properties in visual area V2 of the macaque. Nature *317:*58–61.

Feig, S., and J.K. Harting (1994) Ultrastructural studies of the primate lateral geniculate-nucleus: Morphology and spatial relationships of axon terminals arising from the retina, visual-cortex (area-17), superior colliculus, parabigeminal nucleus, and pretectum of galago-crassicaudatus, J. Comp. Neurol. *343:*17–34.

Fitzpatrick, D., and I.T. Diamond (1980) Distribution of acetylcholinesterase in the geniculo striate system of Galago senegalensis and Aotus trivirgatus: Evidence for the origin of the reaction product in the lateral geniculate body. J. Comp. Neurol. *194:*703–719.

Fitzpatrick, D., K. Itoh, and I.T. Diamond (1983) The laminar organization of the lateral geniculate body and the striate cortex in the squirrel monkey (*Saimiri sciureus*). J. Neurosci. *3:*673–702.

Greenfield, S. (1984) Acetylcholinesterase may have novel functions in the brain. Trends Neurosci. *7:*364–368.

Hanes, M.A., R.T. Robertson, and J. Yu (1992) Transition from mature patterns of acetylcholinesterase activity in visual cortex: Implications for the time course of geniculostriate development. Dev. Brain Res. *66:*97–108.

Hardy, H., L. Heimer, R. Switzer, and D. Watkins (1976) Simultaneous demonstration of horseradish peroxidase and acetylcholinesterase. Neurosci. Lett. *3:*1–5.

Harting, J.K., M.F. Huerta, T. Hashikawa, and D.P. Van Lieshout (1991) Projection of the mammalian superior colliculus upon the dorsal lateral geniculate-nucleus: Organization of tectogeniculate pathways in 19 species. J. Comp. Neurol. *304:*275–306.

Hendrickson, A.E. (1978) The neuroanatomical organization of pathways between the dorsal lateral geniculate nucleus and visual cortex in Old World and New World primates. J. Comp. Neurol. *182:*123–136.

Hendry, S.H.C., and T. Yoshioka (1994) A neurochemically distinct third channel in the macaque dorsal lateral geniculate nucleus. Science *264:*575–577.

Horton, J.C. (1984) Cytochrome oxidase patches: A new cytoarchitectonic feature of monkey visual cortex. Philos. Trans. R. Soc. B (Lond) *304:*199–253.

Horton, J.C., and D.R. Hocking (1996) An adult-like pattern of ocular dominance columns in striate cortex of newborn monkeys prior to visual experience. J. Neurosci. *16:*1791–1807.

Hubel, D., and T.N. Wiesel (1972) Laminar and columnar distribution of geniculo-cortical fibers in the macaque monkey. J. Comp. Neurol. *146:*421–450.

Kennedy, H., J. Bullier, and C. Dehay (1985) Cytochrome oxidase activity in the striate cortex and lateral geniculate nucleus of the newborn and adult monkey. Exp. Brain Res. *61:*204–209.

Kennedy, H., C. Dehay, and G. Horsburgh (1990) Striate cortex periodicity. Nature *348:*494.

Killackey, H.P. (1990) Neocortical expansion: An attempt toward relating phylogeny and ontogeny. J. Cog. Neurosci. *2:*1–17.

Kuljis, R., and P. Rakic (1989) Hypercolumns in primate visual cortex develop in the absence of the cues from the photoreceptors. Proc. Natl. Acad. Sci. USA *87:*5303–5306.

Lachica, E.A., and V.A. Casagrande (1993) The morphology of collicular and retinal axons ending on small relay (W-like) cells of the primate lateral geniculate-nucleus. Vis. Neurosci. *10:*403–418.

Layer, P.G., T. Weikert, and R. Alber (1993) Cholinesterases regulate neurite growth of chick nerve cells in vitro by means of a non-enzymatic mechanism. Cell Tissue Res. *273:*219–226.

Levitt, J.B., T. Yoshioka, and J.S. Lund (1994) Intrinsic cortical connections in macaque visual cortex area V2: Evidence for interaction between different functional streams. J. Comp. Neurol. *342:*551–570.

Levitt, J.B., T. Yoshioka, and J.S. Lund (1995) Connections between the pulvinar complex and cytochrome oxidase-defined compartments in visual area V2 of macaque monkey. Exp. Brain Res. *104:*419–430.

Ling, J., J. Yu, and R.T. Robertson (1995) Sustained inhibition of acetylcholinesterase activity does not disrupt early geniculocortical ingrowth to developing rat visual cortex. Dev. Brain Res. *86:*354–358.

Livingstone, M.S., and D.H. Hubel (1982) Thalamic inputs to cytochrome oxidase-rich regions in monkey visual cortex. Proc. Natl. Acad. Sci. USA *79:*6098–6101.

Livingstone, M.S., and D.H. Hubel (1984) Anatomy and physiology of a color system in primate visual cortex. J. Neurosci. *4:*309–356.

Livingstone, M.S., and D.H. Hubel (1987) Connections between layer 4B of area 17 and the thick cytochrome oxidase stripes of area 18 in the squirrel monkey. J. Neurosci. *7:*3371–3377.

Livingstone, M.S., and D.H. Hubel (1988) Segregation of form, color, movement and depth: Anatomy, physiology and perception. Science *240:*740–749.

Lund, J.S., and R. Boothe (1975) Interlaminar connections and pyramidal neuron organization in the visual cortex of area 17, of the macaque monkey. J. Comp. Neurol. *159:*305–334.

Lund, J.S., A.E. Hendrickson, M.P. Ogren, and E.A. Tobin (1981) Anatomical organization of primate visual cortex area V1. J. Comp. Neurol. *202:*19–45.

Martin, K.A.C. (1988) From enzymes to visual perception: A bridge too far? TINS *11:*380-387.

Nakamura, H., R. Gattass, R. Desimone, and L.G. Ungerleider (1993) The modular organization of projections from areas V1 and V2 to areas V4 and TEO in macaques. J. Neurosci. *13:*3681–3691.

Ogren, M.P., and A.E. Hendrickson (1977) The distribution of pulvinar terminals in visual areas 17 and 18 of the monkey. Brain Res. *137:*343–350.

O'Leary, D.D.M. (1989) Do cortical areas emerge from a protocortex? Trends Neurosci. *12:*400–406.

Rakic, P. (1988) Specification of cerebral cortical areas. Science *241:*170–176.

Rakic, P., I. Suner, and R.W. Williams (1991) A novel cytoarchitectonic area induced experimentally within the primate visual cortex. Proc. Natl. Acad. Sci. USA *88:*2083–2087.

Robertson, R.T., A.A. Tijerina, and M.E. Gallivan (1985) Transient patterns of acetylcholinesterase activity in visual cortex of the rat: Normal development and the effects of neonatal monocular enucleation. Dev. Brain Res. *21:*203–214.

Robertson, R.T., M.A. Hanes, and J. Yu (1988) Investigations of the origins of transient acetylcholinesterase activity in developing rat visual cortex. Dev. Brain Res. *41:*1–23.

Robertson, R.T., F. Mostamand, G.H. Kageyama, K.A. Gallardo, and J. Yu (1991) Primary auditory cortex in the rat: Transient expression of acetylchlolinesterase activity in developing geniculocortical projections. Dev. Brain Res. *58:*81–95.

Rockland, K.S., and D.N. Pandya (1979) Laminar origins and terminations of cortical connections of the occipital lobe in the rhesus monkey. Brain Res. *179:*3–20.

Shipp, S., and S.M. Zeki (1985) Segregation of pathways leading from area V4 to areas V4 and V5 of macaque monkey visual cortex. Nature *315:*322–325.

Shipp, S., and S.M. Zeki (1989) The organization of connections between areas V5 and V2 in macaque monkey visual cortex. Eur. J. Neurosci. *1:*333–354.

Small, D.H. (1990) Non-cholinergic actions of acetylcholinesterases: Proteases regulating cell growth and development? Trends Biochem. *15:*213–216.

Soriano, E., N. Dumesnil, C. Auladell, M. Cohen-Tannoudji, and C. Sotelo (1995) Molecular heterogeneity of progenitors and radial migration in the developing cerebral cortex revealed by transgene expression. Proc. Natl. Acad. Sci USA *92:*11676–11680.

Spatz, W.B., D.M. Voght, and R.B. Illing (1993) Distribution of cytochrome oxidase in layers IV and V of the striate cortex in neonatal monkeys. Exp. Brain Res. *95:*183–186.

Ungerleider, L.G., and M. Mishkin (1982) Two cortical visual systems. In D.J. Ingle, M.A. Goodale, and R.J.R. Mansfield (eds): Analysis of Visual Behavior. Cambridge: MIT Press, pp. 549–586.

Van der Loos, H., and T.A. Woolsey (1973) Somatosensory cortex: Structural alteration following early injury to sense organs. Science *179:*395–398.

Van Essen, D.C., and J.H.R. Maunsell (1980) Two-dimensional maps of the cerebral cortex. J. Comp. Neurol. *191:*255–281.

Van Essen, D.C., W.T. Newsome, J.H.R. Maunsell, and J.L. Bixby (1986) The projections from striate cortex (V1) to areas V2 and V3 in thema-

macaque monkey: Asymmetries, areal boundaries, and patchy connections. J. Comp. Neurol. *244:*451–480.

Weber, J.T., M.F. Huerta, J.H. Kaas, and J.K. Harting (1983) The projection of the lateral geniculate nucleus of the squirrel monkey: Studies of interlaminar zones and the S layers. J. Comp. Neurol. *213:*135–145.

Weller, R.E., and J.H. Kaas (1983) Retinotopic patterns of connections of area 17 with visual area VII and MT in macaque monkeys. J. Comp. Neurol. *220:*253–279.

Wong-Riley, M. (1978) Reciprocal connections between striate and prestriate cortex in the squirrel monkey as demonstrated by combined peroxidase histochemistry and autoradiography. Brain Res. *147:*159–164.

Wong-Riley, M. (1979) Changes in the visual system of monocularly sutured or enucleated kittens demonstrable with cytochrome oxidase histochemistry. Brain Res. *171:*11–28.

Zeki, S.M. (1969) Representation of the central fields on prestriate cortex of monkeys. Brain Res. *14:*271–291.

Zeki, S.M. (1975) The functional organization of projections from striate to prestriate visual cortex in the rhesus monkey. Cold Spring Harbour Symposia on Quantitative Biology *40:*591–600.

Zeki, S.M., and S. Shipp (1988) The functional logic of cortical connections. Nature *335:*311–317.